JCB Article

Nucleocytoplasmic shuttling by nucleoporins Nup153 and Nup214 and CRM1-dependent nuclear export control the subcellular distribution of latent Stat1

Andreas Marg, Ying Shan, Thomas Meyer, Torsten Meissner, Martin Brandenburg, and Uwe Vinkemeier

Abteilung Zelluläre Signalverarbeitung, Leibniz-Forschungsinstitut für Molekulare Pharmakologie, Freie Universität Berlin, 13125 Berlin, Germany

Interferon stimulation of cells leads to the tyrosine phosphorylation of latent Stat1 and subsequent transient accumulation in the nucleus that requires canonical transport factors. However, the mechanisms that control the predominantly cytoplasmic localization in unstimulated cells have not been resolved. We uncovered that constitutive energy- and transport factor-independent nucleocytoplasmic shuttling is a property of unphosphorylated Stat1, Stat3, and Stat5. The NH_2- and COOH-terminal Stat domains are generally dispensable, whereas alkylation of a single cysteine residue blocked cytokine-independent nuclear translocation and thus implicated the linker domain into the cycling of Stat1. It is revealed that constitutive nucleocytoplasmic shuttling of Stat1 is mediated by direct interactions with the FG repeat regions of nucleoporin 153 and nucleoporin 214 of the nuclear pore. Concurrent active nuclear export by CRM1 created a nucleocytoplasmic Stat1 concentration gradient that is significantly reduced by the blocking of energy-requiring translocation mechanisms or the specific inactivation of CRM1. Thus, we propose that two independent translocation pathways cooperate to determine the steady-state distribution of Stat1.

Introduction

The intracellular processing of cytokine signals entails the activation and nuclear translocation of signal transducers and activators of transcription (Stat) factors (Darnell, 1997). Engagement of cytokines with their cognate receptors at the cell membrane triggers the autophosphorylation on tyrosines of noncovalently attached Jak kinases, which also phosphorylate signature tyrosine residues in the intracellular receptor tails (Ihle et al., 1998). This allows receptor binding of the latent Stats via their SH2 domain, and after phosphorylation of a single tyrosine residue at their COOH terminus they form high avidity reciprocal homo- or heterodimers (Shuai et al., 1993, 1994; Greenlund et al., 1995). This sequence of events is commonly referred to as "Stat activation" and within minutes triggers the accumulation of Stat dimers in the nucleus due to their inability to leave this compartment (Meyer et al., 2003, 2004). Here, they can bind to palindromic DNA recognition sites (GAS) and directly induce transcription (Darnell et al., 1994).

The translocation of protein substrates across the nuclear envelope commonly involves transport factors that share homology with the transport factor p97 (also called importin-β; Macara, 2001). These proteins mediate passage of protein cargoes through the nuclear pore complex (NPC; Ryan and Wente, 2000). Based on the direction of cargo transport they have been classified as importins or exportins. The transport process requires metabolic energy and it is propelled by a concentration gradient across the nuclear membrane of the GTP-bound form of the G-protein Ran, which is found predominantly in the nucleus (Görlich and Kutay, 1999). The transport substrates are distinguished in their amino acid sequence by the presence of cis-acting NLS and/or nuclear export signals (NES; Nigg, 1997). Recently, such transport signals were also identified in the Stats. These proteins contain canonical leucine-rich export signals (Begitt et al., 2000; McBride et al., 2000; Bhattacharya and Schindler,

The online version of this article contains supplemental material.

Address correspondence to Uwe Vinkemeier, Abteilung Zelluläre Signalverarbeitung, Leibniz-Forschungsinstitut für Molekulare Pharmakologie, Robert-Rössle-Str. 10, 13125 Berlin, Germany. Tel.: 49-30-94793-171. Fax: 49-30-94793-179. email: vinkemeier@fmp-berlin.de

Key words: Stat1; transcription factor; nuclear transport; nucleoporins; interferon

Abbreviations used in this paper: CIM, complete IM; EDM, energy depletion medium; IM, import mix; LMB, leptomycin B; MBP, maltose-binding protein; NEM, *N*-ethylmaleimide; NES, nuclear export signal; NPC, nuclear pore complex; Nup, nucleoporin; Stat, signal transducer and activator of transcription; TB, transport buffer.

The Journal of Cell Biology, Volume 165, Number 6, June 21, 2004 823–833
http://www.jcb.org/cgi/doi/10.1083/jcb.200403057

The Journal of Cell Biology

2003; Fukuzawa et al., 2003), which are required for binding to the exportin CRM1 (Mattaj and Englmeier, 1998). Because pharmacological or mutational inactivation of the NES–CRM1 pathway does not preclude nuclear export (Begitt et al., 2000), further transport mechanisms for the removal of Stat1 from the nucleus remain to be characterized. In addition, the DNA-binding domain of the Stat1 molecule harbors a dimer-specific NLS (Melén et al., 2001; McBride et al., 2002; Meyer et al., 2002a) that constitutes the binding surface for the adaptor protein NPI-1 of the importin-α family, which tethers the Stat1 protein to the nuclear import factor p97 in a Ran-dependent manner (Sekimoto et al., 1996, 1997; Fagerlund et al., 2002; McBride et al., 2002). Destruction of the dimer-specific NLS precludes nuclear translocation of phosphorylated Stat1 and thus results in the loss of cytokine-inducible transcriptional responses (Meyer et al., 2002a). Surprisingly, unphosphorylated Stat1 can enter the nucleus independently of p97 by an unknown mechanism (Meyer et al., 2002a,b). As generally only molecules of <30 kD can freely cross the NPC by passive diffusion (Paine et al., 1975), the signal-independent nuclear import of unphosphorylated Stats (Mr >87 kD) requires specific interactions with either the NPC or another intermediary carrier.

Here, we examined the behavior of various unphosphorylated Stat proteins in the absence of cytokine stimulation. We found that Stat1, Stat3, and Stat5 can undergo rapid translocation through the nuclear pore in a cytosol-unassisted and carrier-independent manner that does not require metabolic energy. The direct binding of Stat1 to nucleoporins (Nups) indicated that unphosphorylated Stats migrate into the nucleus via specific molecular interactions with components of the NPC. Thus, both carrier-dependent and -independent translocation pathways determine the intracellular distribution of Stat proteins.

Results

Various recombinant Stat proteins were prepared to gain insight into the cytokine-independent nucleocytoplasmic translocation of these transcription factors (Fig. 1). Full-length Stat1 was isolated from baculovirus-infected insect cells. A stable and well-characterized truncated variant, Stat1tc, which lacks both the NH_2 domain of 129 residues and the COOH-terminal transactivation domain of 38 residues was expressed in bacteria (Vinkemeier et al., 1996), as were analogous mutants of Stat3 and Stat5 (Mr >65 kD). The truncated Stat proteins were purified by virtue of a small COOH-terminal Strep-tag, which was also useful for indirect immunocytochemical detection. The recombinant proteins were microinjected into unstimulated cell lines or used for import assays with permeabilized cells. In addition, endogenous Stat1 was targeted by antibody microinjection to reveal the flux rates of the native protein.

Microinjected Stat1, Stat3, and Stat5 rapidly migrate into the nucleus of unstimulated living cells

Several unstimulated cell lines were microinjected into the cytosol with full-length unphosphorylated Stat1. In HeLa-S3 cells (Fig. 2 A), COS7 cells (Fig. 2 B), and 2fTGH cells

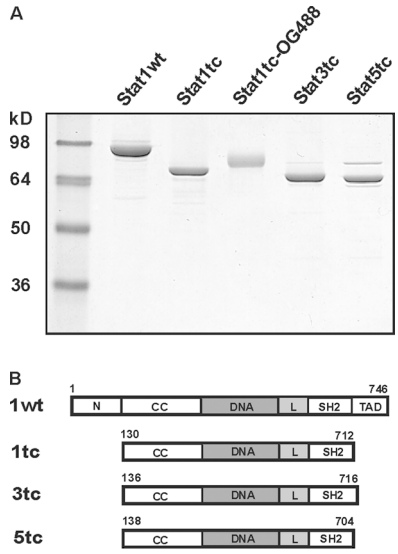

Figure 1. **Recombinant Stat proteins.** (A) SDS-PAGE (7%) analysis of the Stat protein preparations used in this work (1 μg of each). Molecular size markers are indicated to the left. OG488, Oregon green 488. (B) Schematic representation of the respective Stat proteins. The truncated mutants were expressed with a COOH-terminal Strep-tag of the sequence SAWSHPQFEK (single letter code). The Stat proteins were of human (Stat1), mouse (Stat3), or sheep (Stat5) origin. N, N domain; CC, coiled coil domain; DNA, DNA-binding domain; L, linker domain; SH2, SH2 domain; TAD, transactivation domain.

(Fig. 2 C) nuclear import occurred with identical velocity, as it took only 15 min to reach pancellular distribution. Thereafter, no further nuclear accumulation could be observed and the nucleocytoplasmic distribution remained stable (Fig. 2 D). However, treatment of cells with interferon γ for 1 h induced nuclear accumulation of cytoplasmatically microinjected Stat1 (Fig. 2 E). We then compared wild-type Stat1 with a tyrosine phosphorylation-defective mutant (Tyr701Phe) and with truncated Stat1tc. As is shown in Fig. 2 (F and G), nuclear translocation of the two Stat1 variant proteins was indiscriminable from wild-type and also resulted in a pancellular distribution at equilibrium, which indicated that tyrosine phosphorylation as well as NH_2 and COOH termini were dispensable for cytokine-independent nuclear import. Next, we tested the import abilities of truncated Stat3 and Stat5, and found that both proteins enter the nucleus with kinetics similar to Stat1 (Fig. 2, H and I). Notably, the injected Stat3 repeatedly showed a higher steady-state concentration in the nucleus than the two other Stat proteins. In addition, Stat1 and Stat1tc were labeled on lysine residues with fluorescent dyes (either Oregon green 488 or Alexa Fluor 594) to directly observe their nuclear translocation. As is shown in Fig. 2 J for Oregon green 488–labeled Stat1tc, conjugation with fluorescent dyes did not interfere with nuclear import (identical result were obtained with Alexa Fluor 594 and for full-length Stat1; not depicted). However, fluorescent labeling of Stat1 repeatedly caused some material to remain at the cytoplasmic injection site, probably due to precipitation. To demonstrate exclusive passage of the microinjected material through the nuclear pore, we co-injected WGA, a lectin known to inhibit nuclear pore-mediated translocation of macromolecules (Finlay

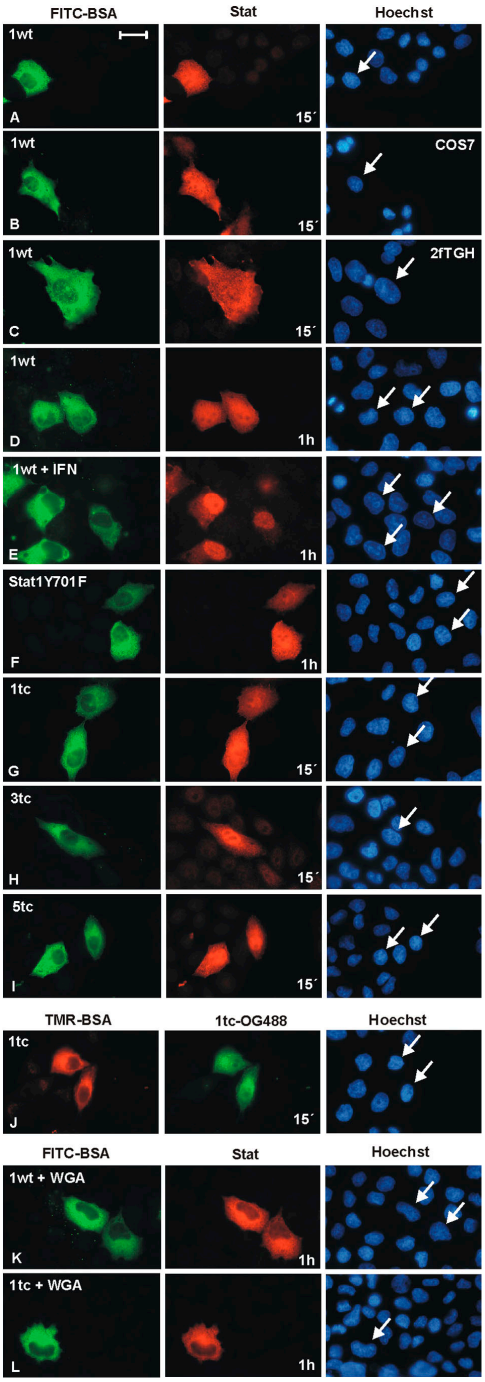

Figure 2. **Unphosphorylated recombinant Stat proteins translocate into the nucleus of unstimulated cells.** HeLa-S3 cells (except for B and C) were used. The injection site is indicated by the location of co-microinjected FITC-labeled or tetramethyl-rhodamine (TMR)–labeled BSA. Nuclei were stained with Hoechst dye. Arrows indicate injected cells. (A–C) Cytoplasmic microinjection of purified Stat1wt into HeLa cells (A) , COS7 cells (B), or 2fTGH cells (C). After 15 min the cells were fixed and Stat1 was detected by immunocytochemistry with a specific antibody. (D) Identical experimental setup as in A, but microinjected cells were fixed after 60 min (E). Identical to D, but cells were treated with IFNγ. (F–I) Cytoplasmic microinjection of full-length tyrosine mutant Y701F (F), or truncated Stat1tc (G), Stat3tc (H), or Stat5tc (I). Fixation was 15 min after injection, truncated Stats were detected with Strep-tag antibody. (J) Cytoplasmic microinjection of Oregon green 488–labeled Stat1tc. Cells were fixed after 15 min followed by direct fluorescence microscopy. (K and L) Cytoplasmic co-microinjection of WGA and Stat1wt (K) or Stat1tc (L). After 1 h the cells were fixed and Stat1 variant proteins were detected by immunocytochemistry as described. Bar, 20 μm.

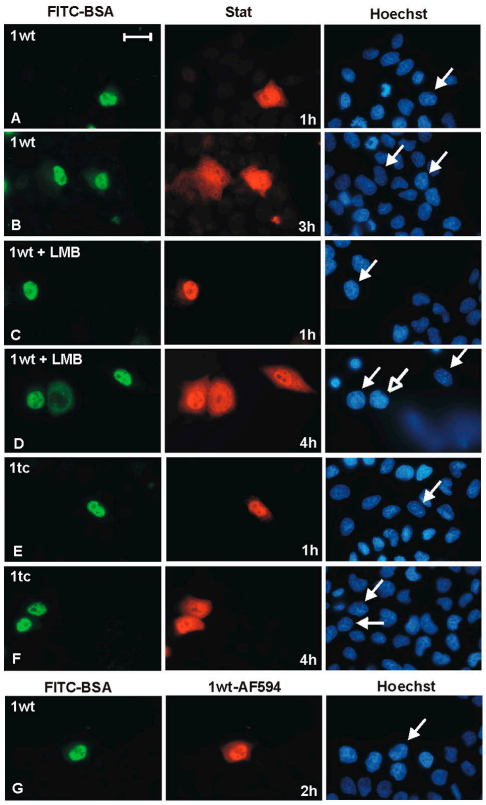

Figure 3. **Unphosphorylated recombinant Stat proteins exit the nucleus of unstimulated cells.** The injection sites of the HeLa cells are indicated by co-microinjected FITC-labeled BSA. (A and B) Recombinant Stat1wt was injected into the nucleus. After 1 h (A) or 3 h (B) immunocytochemistry with a Stat1-specific antibody was performed on fixed cells. (C and D) Microinjection of Stat1wt into cells pretreated for 1 h with LMB. After nuclear (closed arrow) or cytoplasmic (open arrow) microinjection the cells were further incubated with LMB for 1 h (C) or 4 h (D) before fixation and immunocytochemistry with a Stat1-specific antibody. (E and F) Stat1tc was injected into the nucleus and the cells were subsequently incubated for 1 h (E) or 4 h (F), before fixation and immunocytochemistry with Strep-tag antibody. (G) Nuclear microinjection of Alexa Fluor 594–labeled Stat1wt, followed by incubation for 2 h, fixation, and direct fluorescence microscopy. Bar, 20 μm.

et al., 1987). Expectedly, passage across the nuclear envelope of both full-length and truncated Stat1 was effectively blocked (Fig. 2, K and L).

The requirements for the constitutive nuclear import and export of recombinant Stat1 are biochemically distinguishable

Next, recombinant Stat1wt was injected into the nucleus to investigate export kinetics. The microinjected protein quickly left the nucleus and spread evenly across the cell. However, nuclear export appeared to occur slower than nuclear import. It usually took ∼30–60 min to reach a pancellular distribution (Fig. 3 A), which then remained stable (observation for another 2 h; Fig. 3 B). Nuclear export

Table I. **Nucleocytoplasmic translocation of unphosphorylated Stat proteins as determined by microinjection**

	Recombinant Stat[a]		Endogenous Stat[b]	
	GM	EDM	GM	EDM
Import				
1wt	15′	30′	15′	30′
1wt−AF	15′	n.d.	n.a.	n.a.
1tc	15′	30′	n.a.	n.a.
1tc-OG	15′	n.d.	n.a.	n.a.
3tc	15′	30′	n.a.	n.a.
5tc	15′	30′	n.a.	n.a.
Export				
1wt	30′–60′	no export	15′	30′
1wt+LMB	∼4 h	n.d.	n.a.	n.a.
1wt−AF	no export	n.d.	n.a.	n.a.
1tc	∼4 h	n.d.	n.a.	n.a.
1tc+LMB	>4 h	n.d.	n.a.	n.a.
3tc	∼3 h	n.d.	n.a.	n.a.
5tc	∼3 h	n.d.	n.a.	n.a.

GM, growth medium with 10% serum; EDM, serum- and glucose-free EDM with azide and deoxyglucose; n.a., not applicable; n.d., not done; AF, Alexa Fluor 594; OG, Oregon green 488.
[a]Microinjection of recombinant Stat proteins. Listed is the amount of time required to reach equilibrium (min or h).
[b]Microinjection of Stat1 antibodies. Listed are the times required to observe maximal precipitation of endogenous Stat1 in the injected compartment. Each entry represents an averaged value observed by immunocytochemistry in 15–20 microinjected cells after fixation.

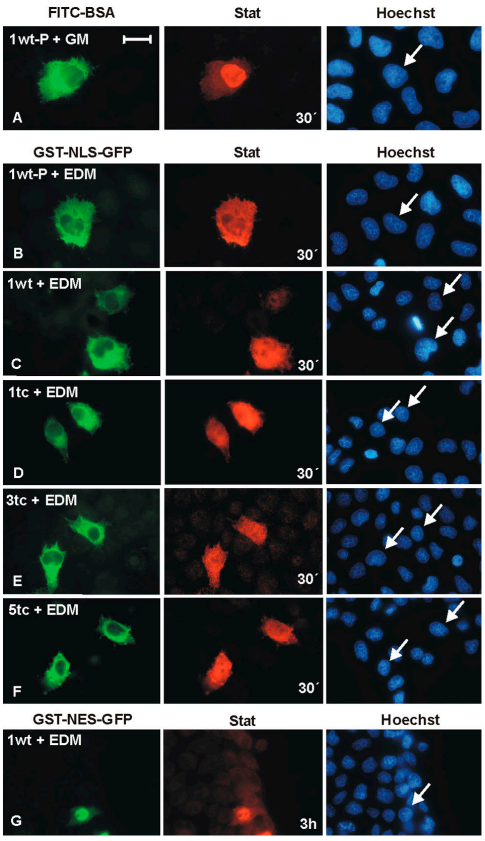

Figure 4. **Unphosphorylated recombinant Stat proteins enter the nucleus of energy-depleted cells.** HeLa cells were kept in growth medium or EDM for 2 h before microinjection. (A and B) Tyrosine-phosphorylated Stat1wt was injected into the cytoplasm of cells treated with growth medium (A) or EDM (B). (C–F) Unphosphorylated Stat1wt (C), Stat1tc (D), Stat3tc (E), or Stat5tc (F) were injected into the cytoplasm of cells incubated in EDM. Injection site and energy depletion are indicated by the location of co-microinjected GST-NLS-GFP. In A, FITC-BSA was used as the injection site marker. The cells were fixed 30 min after injection and Stats were detected by immunocytochemistry. (G) Nuclear co-microinjection of recombinant Stat1wt and GST-NES-GFP, followed by 3 h of incubation in EDM. Then, cells were processed for immunocytochemistry as before. Arrows indicate nuclei of microinjected cells. Bar, 20 μm.

of Stat1 after cytokine-induced nuclear accumulation is achieved in part via the transport receptor CRM1 (Begitt et al., 2000; McBride et al., 2000). It is unclear, however, whether CRM1-dependent nuclear export also functions in the absence of cytokine stimulation. Therefore, cells were treated with the CRM1 inhibitor leptomycin B (LMB; Kudo et al., 1998) starting 60 min before nuclear microinjection. This treatment attenuated nuclear export, because the recombinant protein was still predominantly nuclear after 1 h (Fig. 3 C), and a pancellular distribution was achieved not even after 4 h (Fig. 3 D, closed arrow). Notably, preincubation with LMB followed by cytoplasmic microinjection of Stat1 did not cause its nuclear accumulation (Fig. 3 D, open arrow). These results show that LMB reduces the constitutive nuclear export of Stat1 in unstimulated cells. We have shown in Fig. 2 G that removal of NH_2 and COOH domains did not influence the nuclear import of Stat1. Contrary, nuclear export of the truncated mutant Stat1tc was diminished, because it took about 4 h to achieve an even nucleocytoplasmic distribution (Fig. 3, E and F), and treatment with LMB reduced the export rate even further (Table I). Similar results were obtained also for truncated Stat3 and Stat5 (Table I). Moreover, fluorescently labeled full-length Stat1 was not exported from the nucleus even after 2 h (Fig. 3 G).

The constitutive nuclear import of unphosphorylated recombinant Stat1 continues in energy-depleted cells

Another set of microinjection experiments was performed in living cells that were depleted of ATP by the addition of sodium azide and 2-deoxyglucose. Such treatment was shown to reversibly inhibit classical Ran-dependent nuclear transport by limiting the pool of GTP-bound Ran (Schwoebel et al., 2002). To demonstrate the energy-depleted status of the microinjected cells, we used different injection markers. Here, fusion proteins of GST and GFP that included at their domain junction either a triple SV40 NLS or a Stat1-derived NES (termed GST-NLS-GFP or GST-NES-GFP, respectively) were co-microinjected with recombinant Stat1. The effective nucleocytoplasmic translocation of the reporter constructs was confirmed in cells growing in full-medium (not depicted), whereas preexposure of cells to azide and 2-deoxyglucose for 2 h prevented the carrier-dependent translocation of the reporter protein (Fig. 4, B–G; Fig. 5, E–G). Expectedly, cytoplasmic microinjection of tyrosine-phosphorylated Stat1wt resulted in nuclear accumulation in cells incubated in growth medium (Fig. 4 A), but its nuclear import was prevented in energy-depleted cells (Fig. 4 B).

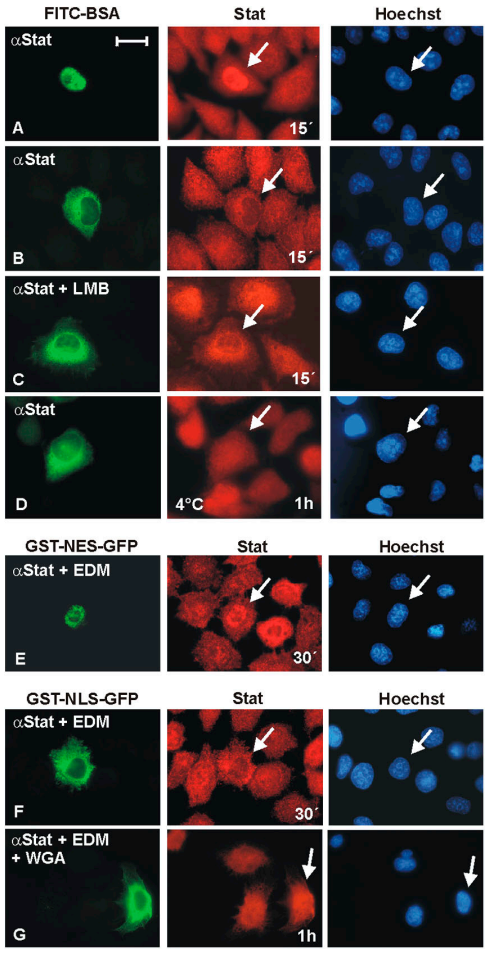

Figure 5. **Nucleocytoplasmic translocation of endogenous Stat1 in normal and energy-depleted HeLa cells.** Stat1 antibodies were microinjected followed by immunocytochemical detection of Stat1. (A) Microinjection of Stat1 antibodies into the cell nucleus with fixation after 15 min. The injection site is marked by co-microinjected FITC-BSA. (B) Identical with A, except that the antibodies were microinjected into the cytoplasm. (C) Identical with B except that the cells were incubated with 5 ng/ml LMB starting 1 h before microinjection. (D) Identical with B, except that the cells were kept at 4° C for 60 min both before and after cytoplasmic microinjection. (E) Stat1 antibodies were microinjected into the nucleus of cells after a 2-h preincubation in EDM. Injection site and energy depletion are indicated by co-microinjected GST-NES-GFP. The cells were fixed 30 min after microinjection. (F and G) Cytoplasmic microinjection of Stat1 antibody in energy-depleted cells. WGA was co-microinjected in G. Injection site and energy depletion are indicated by co-microinjected GST-NLS-GFP. Arrows indicate positions of microinjected cells. Bar, 20 μm.

However, nuclear import of unphosphorylated wild-type (Fig. 4 C) and truncated Stat1 (Fig. 4 D) continued under this condition, albeit at a reduced pace, as it now took ~30 min to reach a pancellular distribution after injection into the cytoplasm. Similarly, nuclear import of recombinant Stat3tc and Stat5tc also continued in energy-depleted cells (Fig. 4, E and F). Notably, the predominantly nuclear localization of Stat3tc seen in cells growing in normal medium was not maintained in ATP-depleted cells (compare Fig. 4 E with Fig. 2 H).

Next, the nuclear export of recombinant wild-type Stat1 and Stat1tc in energy-depleted cells was examined, and it was found that energy depletion blocked the export from the nucleus of both proteins during a 3-h observation period (Fig. 4 G, Stat1wt; compare with Fig. 3, A and B).

Endogenous Stat1 is constitutively shuttling across the nuclear envelope independently of metabolic energy

A different experimental approach was used to investigate the nucleocytoplasmic flux rates also of endogenous Stat1. To this end we performed microinjections of Stat1 antibodies, which has been shown to immobilize the shuttling target antigen and hence cause its accumulation in the microinjected compartment (Meyer et al., 2002a). The results are assembled in Fig. 5 and Table I. As is shown in Fig. 5 A, maximal nuclear accumulation of unphosphorylated Stat1 was seen already 15 min after antibody microinjection into the nucleus. Next, cytoplasmic antibody microinjections were used to estimate the nuclear export rate of the endogenous Stat1 protein. Depletion of nuclear Stat1 was observable as early as 5 min after injection (not depicted), and maximal depletion was achieved with this technique already after 15 min (Fig. 5 B). This assay was also used to determine the inhibitory influence of LMB on the nuclear export of endogenous Stat1. However, the antibody microinjection assay did not allow us to record differences, as the nuclear export rate was not measurably diminished in the presence of LMB (Fig. 5 C). Incubation of the cells at 4°C, however, precluded nuclear export of endogenous Stat1 (Fig. 5 D).

Nuclear import of the endogenous Stat1 continued also during ATP depletion, as revealed after nuclear injection of a Stat1 antibody. Already 15 min past antibody microinjection nuclear accumulation was observable (not depicted), which was maximal after 30 min (Fig. 5 E). We then explored the nuclear export of endogenous Stat1 under these conditions. This was achieved by cytoplasmic co-microinjection of a Stat1 antibody and the GST-NLS-GFP reporter (Fig. 5 F). Clearly, nuclear export of endogenous Stat1 continued in azide/2-deoxyglucose–treated cells, as the nuclear compartment was depleted of Stat1 immunoreactivity after cytoplasmic antibody injection. Co-microinjection of WGA blocked nuclear export, indicating exclusive passage through the nuclear pore also in energy-depleted cells (Fig. 5 G). Energy depletion reduced the transport rate by ~50%, as the time required to clear the nucleus of Stat1 had doubled to 30 min. The nuclear pore is subject to numerous posttranslational modifications such as phosphorylation and glycosylation reactions (Miller et al., 1999). Energy depletion may influence the extent to which the pore proteins are modified, which in turn can modulate transport rates. Together, these results indicated that nucleocytoplasmic shuttling of Stat1 continued in the absence of a physiological Ran-GTP pool.

Exclusively unphosphorylated Stats enter the nucleus of digitonin-permeabilized cells in the absence of cytosol

The behavior of Stat proteins was investigated further with a permeabilized cell transport assay (Adam et al., 1990). HeLa cells were incubated with a concentration of digitonin (40 μg/ml) that selectively permeabilizes the plasma membrane, thereby releasing cytoplasmic proteins. An extensive valida-

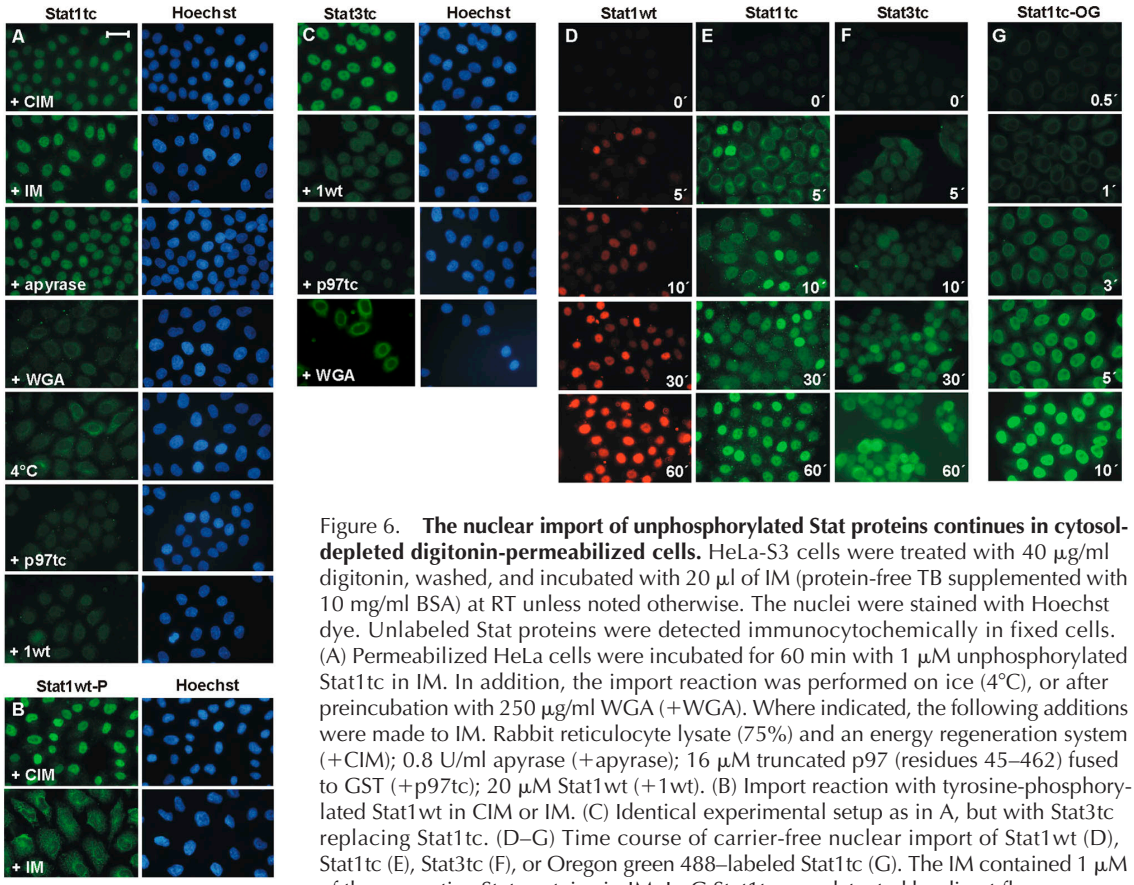

Figure 6. **The nuclear import of unphosphorylated Stat proteins continues in cytosol-depleted digitonin-permeabilized cells.** HeLa-S3 cells were treated with 40 μg/ml digitonin, washed, and incubated with 20 μl of IM (protein-free TB supplemented with 10 mg/ml BSA) at RT unless noted otherwise. The nuclei were stained with Hoechst dye. Unlabeled Stat proteins were detected immunocytochemically in fixed cells. (A) Permeabilized HeLa cells were incubated for 60 min with 1 μM unphosphorylated Stat1tc in IM. In addition, the import reaction was performed on ice (4°C), or after preincubation with 250 μg/ml WGA (+WGA). Where indicated, the following additions were made to IM. Rabbit reticulocyte lysate (75%) and an energy regeneration system (+CIM); 0.8 U/ml apyrase (+apyrase); 16 μM truncated p97 (residues 45–462) fused to GST (+p97tc); 20 μM Stat1wt (+1wt). (B) Import reaction with tyrosine-phosphorylated Stat1wt in CIM or IM. (C) Identical experimental setup as in A, but with Stat3tc replacing Stat1tc. (D–G) Time course of carrier-free nuclear import of Stat1wt (D), Stat1tc (E), Stat3tc (F), or Oregon green 488–labeled Stat1tc (G). The IM contained 1 μM of the respective Stat proteins in IM. In G Stat1tc was detected by direct fluorescence microscopy. Note the different time scale. Bar, 30 μm.

tion of this assay was performed with the carrier-dependent import substrate GFP-NLS-GST. As expected, nuclear import required the addition of cytosol and metabolic energy (Fig. S1, available at http://www.jcb.org/cgi/content/full/jcb.200403057/DC1). A similar analysis was also performed for unphosphorylated Stat1. As is shown in Fig. 6 A, Stat1tc entered the nucleus in the presence of cytosol and metabolic energy (+CIM, complete IM). However, nuclear import was even enhanced in the absence of added exogenous cytosol (Fig. 6 A, +IM, import mix). Pre-treatment of digitonin-permeabilized cells with apyrase to further reduce residual ATP in the absence of added cytosol was without effect on the import of unphosphorylated Stat1tc (Fig. 6 A, +apyrase), in contrast to the tyrosine-phosphorylated proteins Stat1tc (not depicted) and Stat1wt, which required cytosol to enter the nucleus (Fig. 6 B).

Several conditions were found to prevent nuclear import of unphosphorylated Stat1tc in the absence of added cytosol. First, the addition of WGA strongly reduced Stat1 nuclear uptake (Fig. 6 A; +WGA), as did incubation of the permeabilized cells at 4°C (Fig. 6 A, 4°C). To further characterize cytosol-independent nuclear translocation, we examined the saturability of the import process. For this experiment, an NH_2 and COOH terminally truncated fragment of the import receptor p97 was added to the cytosol-free import reaction. This mutant binds irreversibly to proteins of the nuclear pore and thus obstructs multiple import pathways in a dominant fashion (Kutay et al., 1997). As is shown in Fig. 6 A (+p97tc), the inclusion of a 16-fold molar excess of the inhibitory p97 fragment (residues 45–462) completely abrogated nuclear import of Stat1tc. The same result was obtained after adding a 20-fold molar excess of wild-type Stat1 to the import reaction (Fig. 6 A, +1wt).

Cytosol-free import assays with digitonin-permeabilized HeLa cells were successfully performed also with Stat3tc (Fig. 6 C). Because both Stat proteins could enter the nucleus by a carrier-free mechanism, we tested whether they also compete for the same NPC-binding sites. This was done by adding a 20-fold molar excess of wild-type Stat1 to the Stat3tc import reaction, which resulted in a strong suppression of Stat3tc nuclear import (Fig. 6 C, +1wt). Similarly, addition of a 16-fold molar excess of truncated p97 also reduced nuclear import of Stat3tc, as did preincubation with WGA (Fig. 6 C, labeled +p97tc and +WGA, respectively).

To estimate the nuclear entry rates of Stat1wt and truncated Stat1 and Stat3 in digitonin-permeabilized cells, a time course experiment was performed. As is shown in Fig. 6 (D–F), all three proteins entered the nucleus with similar kinetics. Already after 5 min the Stat proteins were detectable at the nuclear rim and inside some nuclei, and after 10 min the Stats had accumulated in most of the nuclei. The accumulation phase continued and reached a plateau between 30 and 60 min. Interestingly, we noted that the import rate of Stat1 and Stat3 differed among individual nuclei (Fig. 6, D–F). Incorrect cell permeabilization leading to rupturing of the nuclear membrane is an unlikely explanation for this be-

cause staining of digitonin-permeabilized cells with labeled Con A was limited to the cell membrane (unpublished data; Dean and Kasamatsu, 1994). Moreover, the cytosol-free nuclear import of p97 did not differ among individual nuclei of permeabilized cells (Fig. S1 B; Kose et al., 1997; Miyamoto et al., 2002). Of note, fluorescent labeling increased both the transport rate and the homogeneity of Stat1 nuclear import (Fig. 6 G). We also attempted to establish cytosol-free nuclear import for Stat5tc. Although ~10% of the nuclei showed nuclear import of Stat5tc, the remaining cells displayed strong labeling in the extranuclear space of what appeared to constitute precipitated Stat5tc protein (unpublished data).

These results indicate that Stat1, Stat3, and Stat5 have the ability to migrate into the nucleus by themselves in the absence of metabolic energy or added transport factors. They share binding partners in the NPC among each other and with the import receptor p97.

Stat1 binds to Nup153 and Nup214, but not Nup62

The above data are not compatible with a carrier-mediated nuclear translocation process. Rather, they are characteristic for a carrier-free mechanism that occurs through direct interactions between the Stats and constituents of the nuclear pore. A distinctive feature of numerous NPC proteins is the presence of Phenylalanine/Glycine (FG)-rich repeat motifs, which provide interaction sites for transport factors (Ryan and Wente, 2000). Because Stats and p97 appeared to share binding sites on nuclear pore proteins, we examined whether Stat1 could also interact with constituents of the nuclear pore. FG repeat–containing parts of His-tagged Nup214 (residues 1549–2090), Nup62 (residues 1–308), and Nup153 (residues 333–618; the latter two were fusion proteins with maltose-binding protein; MBP) were expressed in bacteria and detected by immunoblotting with the mAb 414 (Davis and Blobel, 1986; Fig. S2, available at http://www.jcb.org/cgi/content/full/jcb.200403057/DC1). The bacterial lysates were resolved by denaturing SDS-PAGE (Fig. 7, bottom) and subsequently blotted on nitrocellulose. After extensive incubation in renaturing buffer, the immobilized proteins were incubated with wild-type Stat1, the binding of which was detected by Western blotting (Fig. 7, top). No binding of Stat1 was seen with MBP and a His-tagged control protein, but Stat1 bound strongly to both Nup214 and Nup153. Contrary, no binding was detected to the FG repeat region of Nup62. These results suggested that Stat1 is able to bind directly to the FG repeat region of Nup153 and Nup214, supporting a model in which unphosphorylated Stat1 engages in carrier-free nucleocytoplasmic shuttling through direct interactions with components of the nuclear pore.

The linker domain of Stat1 plays a role in cytokine-independent nuclear translocation

Stat1 contains highly reactive cysteine residues which can cause aggregation of recombinant purified protein (Vinkemeier et al., 1996). This problem can be overcome by blocking reactive SH-groups with *N*-ethylmaleimide (NEM), which has been shown to leave in vitro DNA binding undisturbed (Vinkemeier et al., 1996). However, when truncated

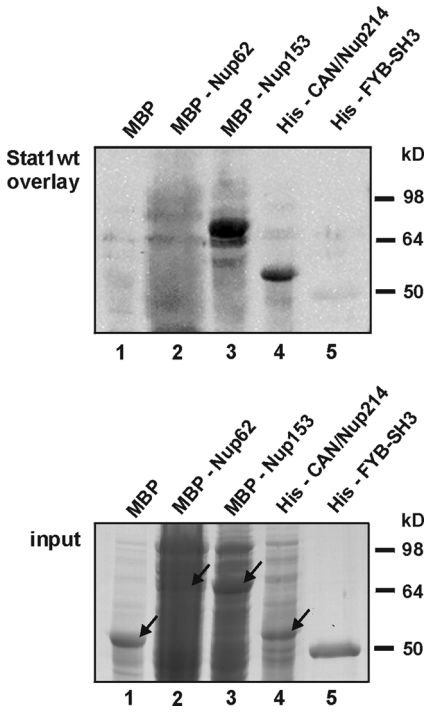

Figure 7. **Stat1 interacts with FG repeat–containing Nups.** (Top) Bacterial lysates containing the indicated fusion proteins (lanes 1–4) or purified His-tagged tandem SH3 domains from FYB (lane 5) were resolved by SDS-PAGE, transferred to a nitrocellulose membrane, and probed with wild-type unphosphorylated Stat1. The association of Stat1 with the immobilized proteins was detected by immunoblotting using a Stat1-specific antibody. The bottom panel shows the respective Coomassie-blue stained SDS-gel before transfer to a nitrocellulose membrane (input). Arrows indicate the proteins listed above the respective lane.

Stat1 was alkylated and microinjected into cells, we could no longer detect nucleocytoplasmic shuttling, as both import and export (not depicted) were strongly diminished (Fig. 8 A). Mutation of eight out of the nine cysteine residues of human Stat1tc prevented NEM from inhibiting nuclear import (Fig. 8 D), indicating that cysteine alkylation caused the inhibitory effect. Further experiments unambiguously demonstrated that mutation of Cys543, which is located in the linker domain, was responsible for rescuing Stat1 from the shuttling defects caused by NEM (Fig. 8 B). Mutation of other cysteine residues did not prevent NEM from inhibiting nuclear translocation of Stat1 (Fig. 8 C, Cys492). Mass spectrometry confirmed alkylation of recombinant Stat1tc in position 8 (Cys543), and also of positions 5 (Cys324) and 9 (Cys577) (Fig. 8 D). Interestingly, mutation to alanine or arginine of residue 543 was without adverse effects on nuclear import (unpublished data). On the other hand, mass spectrometric analysis revealed that full-length Stat1 was not alkylated by NEM in position 543, and treatment with NEM was thus without effect on its nuclear import (unpublished data).

Carrier-dependent and -independent pathways cooperatively determine the subcellular distribution of Stat1 in resting cells

It is currently unknown how the Stats achieve their predominantly cytoplasmic localization in unstimulated cells. As is

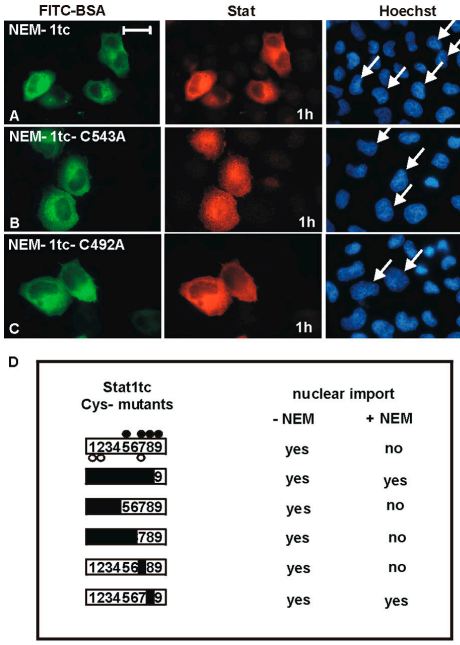

Figure 8. **Alkylation of cysteine 543 in the linker domain precludes nuclear import of Stat1.** (A–C) Purified Stat1tc or the indicated mutants were alkylated by NEM in vitro and injected in the cytosol of HeLa cells. After 1 h the cells were fixed and the intracellular distribution of the microinjected proteins was determined by immunocytochemistry. Arrows indicate nuclei of microinjected cells. Bar, 20 μm. (D) Summary of the microinjection data and mass spectrometric analyses of alkylated Stat1. Purified bacterially expressed Stat1tc was treated without or with NEM (Materials and methods) and subsequently injected into the cytoplasm of HeLa cells. The ability to enter the nucleus during a 1-h incubation period is stated. The cysteine residues in position 155, 174, 247, 255, 324, 440, 492, 543, 577 of human Stat1 are numbered 1 to 9 in the diagram to the left. Mutated cysteines (Cys to Ala) are blackened. Open circles denote absence of alkylation; closed circles denote alkylated cysteines as determined by mass spectrometry. For position 7 both alkylated and nonalkylated peptides were found. Peptides covering Cys-positions 3, 4, and 6 were not detected.

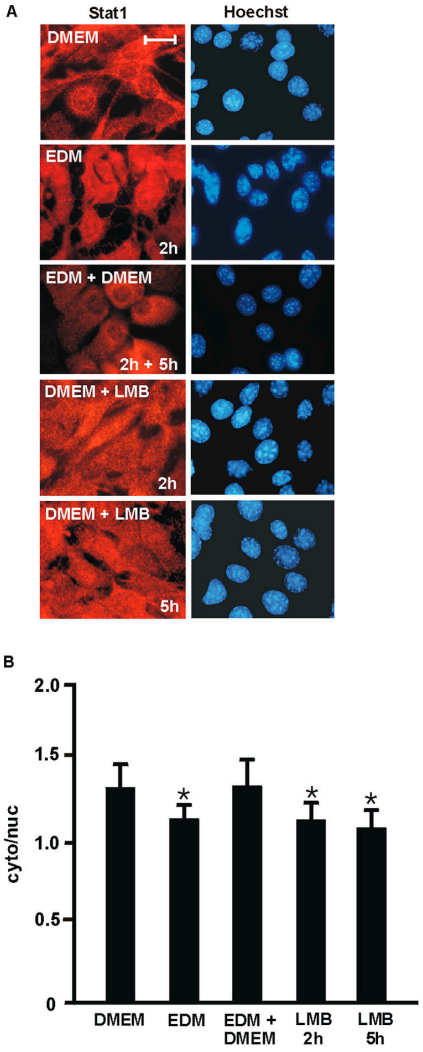

Figure 9. **The inhibition of active nuclear export prevents cytoplasmic accumulation of Stat1.** (A) 3T3 cells were left untreated (DMEM) or treated with EDM for 2 h followed by growth medium for 5 h (EDM+DMEM). Alternatively, cells were treated with the CRM1 inhibitor leptomycin B (LMB) for 2 or 5 h as indicated. Shown is the distribution of the endogenous Stat1 as revealed by immunocytochemistry with a specific antibody and conventional microscopy. Bar, 20 μm. (B) Corresponding bar diagram with a quantitative analysis of the ratio of the mean cytoplasmic and nuclear immunofluorescence densities. The median slice (x/y image) of a confocal microscopical image was used to quantify the signals in 13 randomly chosen cells Values are expressed as mean ± SD. Statistically significant differences between cells incubating in control (DMEM) or experimental medium are indicated by the asterisks.

shown above, before stimulation with cytokines Stat1 enters the nucleus independent of metabolic energy and transport factors. Export of Stat1 from the nucleus, however, can occur via two pathways, only one of which functions without metabolic energy, whereas the second pathway requires an NES, the exportin CRM1 and metabolic energy (Begitt et al., 2000; McBride et al., 2000). Therefore, we used energy depletion and used the specific CRM1 inhibitor LMB to suppress the NES-dependent active nuclear export of Stat1. As is shown in Fig. 9 A, exposure of 3T3 cells to energy depletion medium (EDM) for 2 h reduced the cytoplasmic accumulation of Stat1, and a statistically significant relocation to the nucleus resulting in a pancellular distribution was observed (Fig. 9 B). Expectedly, the nuclear relocation of Stat1 was reversible, because the subsequent incubation in full growth medium for 5 h restored the cytoplasmic accumulation of Stat1 (Fig. 9 A). Treatment of cells with the CRM1 inhibitor LMB also caused relocalization and pancellular distribution of Stat1. Importantly, prolonged exposure to LMB for 5 h had the same effects and did not induce nuclear accumulation (Fig. 9, A and B).

Discussion

Here, we have investigated both in vitro and in vivo the nucleocytoplasmic translocation of Stats before their activation. The results shown here reveal that unphosphorylated Stat1, Stat3, and Stat5 are shuttling proteins that rapidly traverse the nuclear envelope. Several lines of evidence indicated that this is a process distinct from the conventional import mechanism described for tyrosine-phosphorylated Stat1 (Fig. 10). (a) All transport processes known to date that depend on transport factors rely on metabolic energy in vivo (Görlich and Kutay, 1999). Nuclear translocation of

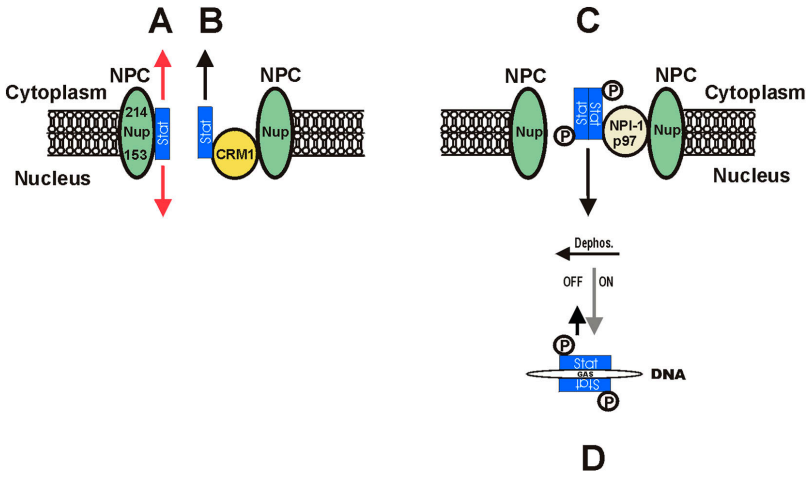

Figure 10. **A model of Stat1 nucleocytoplasmic shuttling.** (A) Unphosphorylated "latent" Stat1 constitutively shuttles between cytosol and nucleoplasm via direct interactions with the Nup153 and Nup214. The surface of the linker domain of Stat1 is likely to provide the contact surface. (B) In addition, NES-mediated transport of unphosphorylated Stat1 via CRM1 enhances the export rate and achieves cytoplasmic accumulation. (C) After cytokine-induced receptor activation, Stat1 is tyrosine phosphorylated and dimerizes, which precludes further carrier-free nucleocytoplasmic cycling. However, a dimer-specific NLS in the DNA-binding domain is exposed, and nuclear import occurs in complex with NPI-1 and p97. (D) Until its dephosphorylation, which is inhibited by DNA-binding, Stat1 is retained in the nucleus, thus allowing for the signal-induced nuclear accumulation. GAS, Stat1-binding site.

unphosphorylated Stat1, Stat3, and Stat5, however, continued in energy-depleted cells, whereas the translocation of tyrosine-phosphorylated Stat1 or of a transport factor-dependent reporter construct did not (Fig. 4; Fig. 5, E and F). (b) Nuclear import of unphosphorylated Stat1 and Stat3 was readily observable in digitonin-permeabilized cells in the absence of added cytosol (Fig. 6, A and C). Contrary, tyrosine-phosphorylated Stat1 or a p97-dependent reporter construct could not enter the nucleus in this system (Fig. 6 B and Fig. S1 A). (c) Unphosphorylated Stat1 was demonstrated to directly interact with the FG repeat region of Nup153 and Nup214, but not Nup62 (Fig. 7). These results are compatible with a model describing nucleocytoplasmic translocation of unphosphorylated Stats as a carrier-independent process that relies on direct interactions between Stat proteins and the nuclear pore (Fig. 10). The carrier-free nuclear import of the Stats is rapid and saturable. Nuclear import in digitonin-permeabilized cells or after cytoplasmic microinjection was detectable already after 5 min, and trapping of endogenous Stat1 by antibody microinjection in the nucleus of resting HeLa cells resulted in nuclear accumulation after ~15 min. Contrary to the results presented here for wild-type Stat1, examination of GFP-tagged Stat1 with fluorescence loss in photobleaching indicates that the nuclear and cytoplasmic pools do not exchange rapidly (Lillemeier et al., 2001). However, in unstimulated cells GFP-tagged Stat1 traverses the nuclear membrane much less efficiently in comparison to the wild type (unpublished data).

Active nuclear export has been demonstrated to participate in the termination of the interferon-induced nuclear accumulation of Stat1 (Begitt et al., 2000; McBride et al., 2000). Here, we extend these data and show that both active, CRM1-dependent and carrier-free nuclear export occur simultaneously regardless of cytokine stimulation, as indicated by the protracted export of nuclear-microinjected Stat1 during LMB treatment (Fig. 3, C and D). The nuclear import of unphosphorylated Stat1, on the other hand, appears to occur via a carrier-free process, because the specific inactivation of CRM1-mediated export did not cause nuclear accumulation (Fig. 3 D). In addition, no evidence for a functional NLS was found in unphosphorylated Stat1 (Sekimoto et al., 1997; Begitt et al., 2000; Meyer et al., 2002a; Ma et al., 2003). Therefore, we propose a model in which diffusion-controlled import and energy-consuming export contribute to the observed accumulation of Stat1 in the cytoplasm of unstimulated cells. In line with this model we found that the cytoplasmic accumulation of Stat1 was significantly diminished upon ATP depletion or exposure of resting cells to the CRM1 inhibitor LMB (Fig. 9). Similar observations were previously made also for Stat2, Stat3, and Stat5 (Rodriguez et al., 2002; Zeng et al., 2002; Bhattacharya and Schindler, 2003). Thus, we conclude that the influx rate of Stat1 into the nuclei of unstimulated cells is influenced by its concentration gradient between cytosol and nucleoplasm. However, the Stat proteins are likely to differ in the extent to which these pathways determine their overall transport rate. Contrary to Stat1, a constitutive carrier-dependent import signal was described for Stat3 (Ma et al., 2003). Accordingly, the cytoplasmic microinjection of Stat3tc resulted in its nuclear accumulation (Fig. 2 H), but an even nucleocytoplasmic distribution resulted if the cells were cultured in EDM (Fig. 4 E).

The structural requirements that enable the nucleocytoplasmic shuttling of unphosphorylated Stats are complex. Similar to observations that were previously made with importin p97, where alkylation with NEM precluded binding to the nuclear pore (Chi and Adam, 1997), also the translocation of Stat1 was sensitive to NEM. Alkylation of a single variant cysteine residue in the linker domain precluded nuclear translocation and thus implicated this rather nondescript region of Stat1 in nuclear transport. Further work is also necessary to explore the role of the Stat NH_2 and COOH domains, which were dispensable for nuclear import, but the presence of which accelerated nuclear export. These observations as well as the competition data, which indicated that the Stat proteins share NPC-binding sites among themselves and with p97 (Fig. 6, A and C) raise the issue of specificity in carrier-free protein translocation. Besides the truncation of Stats, several other conditions affected transport in a direction-specific manner. Energy depletion and fluorescent labeling specifically blocked the nuclear export of recombinant Stat1. Also, for unknown reasons the import rates of both Stat1 and Stat3 differed among individual nuclei of digitonin-permeabilized cells. Addition of ATP, which remedied a similar problem in carrier-free nuclear translocation of importin-α (Miyamoto et al.,

2002), or using recombinant protein from insect cells instead of bacteria had no effect on nuclear import (unpublished data). However, labeling of Stat1 with fluorescent dyes, while preventing export (Fig. 3 G), made nuclear import more homogenous (Fig. 6 G). Of note, several experiments indicated that the shuttling rate of endogenous Stat1 exceeded that of the microinjected recombinant protein (Table I). Therefore, it is conceivable that posttranslational modifications influence the translocation through the nuclear pore, possibly even in a direction-specific manner. Such mechanisms could also account for cell type or Stat-specific differences in the subcellular distribution of members of this protein family.

In summary, our results demonstrate that the steady-state distribution of Stat proteins is maintained by diverse transport mechanisms both before and after cytokine stimulation of cells. Thus, in light of the constant cycling that characterizes the Stat transcription factors, the cytokine signal transduction is best described as a "continuous signaling cycle" rather than a linear pathway that starts at the cell membrane and ends in the nucleus.

Materials and methods

Cell culture and energy depletion

Cells were grown in complete growth medium as described previously (Begitt et al., 2000). 5 ng/ml LMB (Sigma-Aldrich) was added to the cells 60 min before microinjection. For energy depletion studies, HeLa-S3 or NIH-3T3 cells were washed with PBS, and incubated in serum- and glucose-free DME (GIBCO BRL). This medium was supplemented with 10 mM sodium azide and 10 mM 2-deoxy-*D*-glucose (EDM) and left on the washed cells for 2 h. Subsequently, the cells were either fixed in methanol for 6 min at −20°C, or microinjected with antibodies or recombinant protein and the incubation in EDM was continued for the indicated times. Alternatively, after 2 h in EDM the cells were kept in complete growth medium for 5 h before fixation. Stat1 was detected by immunocytochemistry with 0.2 μg/ml of antibody E-23 (Santa Cruz Biotechnology, Inc.).

Plasmids and mutagenesis

For expression in bacteria, the cDNAs encoding truncated human Stat1 (aa 130–712), mouse Stat3 (aa 136–716), or sheep Stat5 (aa 138–704) were amplified by PCR and cloned into the EcoRI and BamHI sites of pASKIBA3 (IBA). The cDNA encoding aa 45–462 of p97 was PCR-amplified and cloned into pGEX-5X-2 (Amersham Biosciences). MBP fusion proteins of the FG repeat regions of human Nup62 (aa 1–308; a gift of E. Hurt, Universität Heidelberg, Heidelberg, Germany) and human Nup153 (aa 333–618; a gift of B.K. Felber, National Cancer Institute, Frederick, MD) were prepared after PCR amplification of the respective cDNAs and cloning into the BamHI site of pMal-2CX (NEB). PCR reactions were performed with Vent-proofreading polymerase (NEB). Site-directed mutagenesis was performed with the Quick-change kit (Stratagene). Baculovirus transfer vectors (pFastBac) encoding human Stat1wt (aa 1–746) or the Tyr701Phe mutant and vectors for bacterial expression of GST-NLS-GFP and GST-NES-GFP have been described previously (Meyer et al., 2003). Expression constructs for His-tagged human p97 (aa 1–878) and human Nup214 (aa 1549–2090) were gifts of U. Kutay (ETH Zürich) and M. Fornerod (Nederlands Kanker Instituut, Amsterdam, Netherlands), respectively.

Expression, purification, alkylation, and fluorescent labeling of recombinant proteins

Expression of Stat1wt and Stat1Y701F in baculovirus-infected Sf9 insect cells, the purification and tyrosine phosphorylation were done as described previously (Meyer et al., 2003). Protein expression in BL21p(Lys)S bacteria was induced at an OD_{600} of 0.8 with 1 mM anhydrotetracycline (Acros, pASKIBA3 vector), or IPTG (1 mM for pGEX and 0.3 mM for pMal vectors, respectively). Protein expression was at 18°C for 15 h (Strep-tagged proteins), or at 30°C for 5 h or 3 h with GST- or MBP-tagged proteins, respectively. Cells were lysed by sonication in PBS containing 0.1% Triton X-100, 2 mM EDTA, 2 mM EGTA, 5 mM DTT. Proteins were single-step purified by virtue of their Strep- or GST-tag, respectively, as recommended by the manufacturers (IBA; Amersham Biosciences). Where indicated, purified proteins were alkylated with 20 mM NEM as described previously (Vinkemeier et al., 1996). Proteins were concentrated by ultrafiltration (Centriprep; Millipore) in injection buffer containing 5 mM DTT (Meyer et al., 2002a); protein concentrations were determined by UV spectroscopy (extinction coefficient 1.25 for Stat1wt, 1.27 for Stat1tc, 1.24 for Stat3tc, and 1.43 for Stat5tc; Vinkemeier et al., 1996), or by Coomassie dye binding (Bio-Rad Laboratories) with a BSA standard. Proteins were quick frozen on dry ice and stored at −80°C. Fluorescence labeling of Stat1wt and Stat1tc was done with succinimidyl esters of Alexa Fluor 594 or Oregon green 488 as described by the manufacturer (Molecular Probes) at a molar protein/dye ratio of 1:5. Efficiency of labeling was close to 100% as judged by mobility shift in SDS-PAGE (Fig. 1). His-tagged p97 was expressed and purified as described previously (Kutay et al., 1997).

Microinjection

Microinjections of antibodies (at 0.15 mg/ml in PBS) and concentrated recombinant proteins (at 0.5–1 mg/ml) were done as described previously (Meyer et al., 2002a). Injection site markers were used at a concentration of 0.5–1 mg/ml; WGA (Sigma-Aldrich) was co-microinjected at a concentration of 0.5 mg/ml. Immunocytochemistry was with monoclonal Stat1 antibody C-136 (0.2 μg/ml; Santa Cruz Biotechnology, Inc.) or anti-Strep-tag II rabbit pAb (0.2 μg/ml; IBA).

Import assays with permeabilized cells

Adherent HeLa-S3 cells were grown on poly-L-lysine–coated coverslips and permeabilized with 40 μg/ml digitonin (Roche) in transport buffer (TB; 20 mM Hepes, pH 7.3, 110 mM KOAC, 2 mM $Mg(OAC)_2$, 1 mM EGTA, 2 mM DTT, complete protease inhibitors [Roche]) for 5 min at RT followed by 5 min on ice (Adam et al., 1990). Subsequently, the cells were washed in TB twice. Incubation with 20 μl import mix (IM) was performed at RT for 60 min or as indicated. The cytosol-free IM contained TB supplemented with 10 mg/ml BSA and one or several of the following purified proteins as indicated: 1 μM Stat1tc, 1 μM Stat3tc, 1 μM Stat5tc, 1 μM Oregon green 488– or Alexa Fluor 594–labeled Stat1tc, 15 μM Stat1wt, 0.8 μM GST-NLS-GFP, or 0.8 μM full-length His-tagged p97. The complete IM (CIM) contained 75% (vol/vol) rabbit reticulocyte lysate (Promega) that included an energy regenerating system (0.5 mM ATP, 0.5 mM GTP, 10 mM creatine phosphate, 30 U/ml creatine phosphokinase), and 25% IM. For WGA treatment, digitonin-permeabilized cells were incubated for 10 min on ice in IM containing 250 μg/ml WGA or as indicated, before washing and addition of the IM. For ATP depletion, IM or CIM were preincubated for 15 min on ice in the presence of 0.8 U/ml apyrase (Sigma-Aldrich) before addition to the permeabilized cells. For competition assays, 16 μM truncated p97 (aa 45–462) or 20 μM full-length Stat1 was added to IM and left on the cells for 45 min. After the import reaction the cells were washed with ice-cold TB and fixed for 10 min at RT with 3.7% PFA in PBS, before permeabilization with 0.2% Triton X-100 in PBS (2 min at RT). Truncated Stats were detected with 0.17 μg/ml of Strep-tag II antibody; for Stat1wt antibody C-136 was used (0.07 μg/ml); and His-tagged p97 was detected with 0.25 μg/ml of anti-His antibody (Abcam). Fixed cells were mounted in TB containing 50% glycerol, 0.1% (wt/vol) NaN_3, 1% (wt/vol) Diazobicyclo (2,2,2)-odone.

In vitro binding assay

Bacterial lysates (containing ∼6 μg NPC proteins or MBP) and 6 μg purified His-tagged control protein (tandem SH3 domains from human FYB; a gift of C. Freund, Freie Universität Berlin) were resolved by 10% SDS-PAGE and transferred to a nitrocellulose membrane. The membrane was rinsed in TB (20 mM Hepes, pH 7.4, 110 mM KOAc, 2 mM $Mg(OAc)_2$, 0.5 mM EGTA, 2 mM DTT, 0.5% Tween-20, complete protease inhibitors), and then blocked in this buffer plus 5% (wt/vol) nonfat milk for 1 h at 4°C. Recombinant full-length Stat1 was added at 3 μg/ml, and the incubation continued for 16 h at 4°C. Subsequently the blot was rinsed three times with TB and subjected to Western analysis using anti-Stat1 antibody C-136 (0.2 μg/ml).

Fluorescence microscopy and fluorescence quantification

Conventional and confocal fluorescence analysis and quantification of immunofluorescence intensities were performed as described previously (Meyer et al., 2002b). The data were analyzed by ANOVA followed by Tukey multiple comparison tests. Differences were considered statistically significant at $P < 0.05$.

Online supplemental material

Fig. S1 A shows that a carrier-dependent control protein requires cytosol for nuclear import into digitonin-permeabilized HeLa cells. In B the cyto-

sol-independent nuclear import of p97 is demonstrated. Fig. S2 shows immunoblotting results with the FG repeat–specific antibody 414 and bacterial lysates containing recombinant Nups. Online supplemental material is available at http://www.jcb.org/cgi/content/full/jcb.200403057/DC1.

This work is dedicated to Professor Klaus Weber in honor of his emeritation.

We wish to acknowledge M. Kummerow for expert technical assistance, and E. Krause for mass spectrometry. Useful reagents were provided by B.K. Felber, C. Freund, M. Fornerod, E. Hurt, and U. Kutay.

This work was supported by grants from the Deutsche Forschungsgemeinschaft, the Bundesministerium für Bildung und Forschung (BioFuture), the EMBO-Young-Investigator Program (to U. Vinkemeier), and a predoctoral fellowship by Boehringer Ingelheim Fonds (to T. Meissner).

Submitted: 8 March 2004
Accepted: 7 May 2004

References

Adam, S.A., R.S. Marr, and L. Gerace. 1990. Nuclear protein import in permeabilized mammalian cells requires soluble cytoplasmic factors. *J. Cell Biol.* 111: 807–816.

Begitt, A., T. Meyer, M. van Rossum, and U. Vinkemeier. 2000. Nucleocytoplasmic translocation of Stat1 is regulated by a leucine-rich export signal in the coiled-coil domain. *Proc. Natl. Acad. Sci. USA.* 97:10418–10423.

Bhattacharya, S., and C. Schindler. 2003. Regulation of Stat3 nuclear export. *J. Clin. Invest.* 111:553–559.

Chi, N.C., and S.A. Adam. 1997. Functional domains in nuclear import factor p97 for binding the nuclear localization sequence receptor and the nuclear pore. *Mol. Biol. Cell.* 8:945–956.

Darnell, J.E., Jr. 1997. Stats and gene regulation. *Science.* 277:1630–1635.

Darnell, J.E., Jr., I.M. Kerr, and G.R. Stark. 1994. Jak-Stat pathways and transcriptional activation in response to IFNs and other extracellular signaling proteins. *Science.* 264:1415–1421.

Davis, L.I., and G. Blobel. 1986. Identification and characterization of a nuclear pore complex protein. *Cell.* 45:699–709.

Dean, D.A., and H. Kasamatsu. 1994. Signal- and energy-dependent nuclear transport of SV40 Vp3 by isolated nuclei. Establishment of a filtration assay for nuclear protein import. *J. Biol. Chem.* 269:4910–4916.

Fagerlund, R., K. Melén, L. Kinnunen, and I. Julkunen. 2002. Arginine/lysine-rich nuclear localization signals mediate interactions between dimeric Stats and importin alpha 5. *J. Biol. Chem.* 277:30072–30078.

Finlay, D.R., D.D. Newmeyer, T.M. Price, and D.J. Forbes. 1987. Inhibition of in vitro nuclear transport by a lectin that binds to nuclear pores. *J. Cell Biol.* 104:189–200.

Fukuzawa, M., T. Abe, and J.G. Williams. 2003. The Dictyostelium prestalk cell inducer DIF regulates nuclear accumulation of a Stat protein by controlling its rate of export from the nucleus. *Development.* 130:797–804.

Görlich, D., and U. Kutay. 1999. Transport between the cell nucleus and the cytoplasm. *Annu. Rev. Cell Dev. Biol.* 15:607–660.

Greenlund, A.C., M.O. Morales, B.L. Viviano, H. Yan, J. Krolewski, and R.D. Schreiber. 1995. Stat recruitment by tyrosine-phosphorylated cytokine receptors: an ordered reversible affinity-driven process. *Immunity.* 2:677–687.

Ihle, J.N., W. Thierfelder, S. Teglund, D. Stravapodis, D. Wang, J. Feng, and E. Parganas. 1998. Signaling by the cytokine receptor superfamily. *Ann. NY Acad. Sci.* 865:1–9.

Kose, S., N. Imamoto, T. Tachibana, T. Shimamoto, and Y. Yoneda. 1997. Ran-unassisted nuclear migration of a 97-kD component of nuclear pore-targeting complex. *J. Cell Biol.* 139:841–849.

Kudo, N., B. Wolff, T. Sekimoto, E.P. Schreiner, Y. Yoneda, M. Yanagida, S. Horinouchi, and M. Yoshida. 1998. Leptomycin B inhibition of signal-mediated nuclear export by direct binding to CRM1. *Exp. Cell Res.* 242: 540–547.

Kutay, U., E. Izaurralde, F.R. Bischoff, I.W. Mattaj, and D. Görlich. 1997. Dominant-negative mutants of importin-beta block multiple pathways of import and export through the nuclear pore complex. *EMBO J.* 16:1153–1163.

Lillemeier, B.F., M. Köster, and I.M. Kerr. 2001. STAT1 from the cell membrane to the DNA. *EMBO J.* 20:2508–2517.

Ma, J., T. Zhang, V. Novotny-Diermayr, A.L. Tan, and X. Cao. 2003. A novel sequence in the coiled-coil domain of Stat3 essential for its nuclear translocation. *J. Biol. Chem.* 278:29252–29260.

Macara, I.G. 2001. Transport into and out of the nucleus. *Microbiol. Mol. Biol. Rev.* 65:570–594.

Mattaj, I.W., and L. Englmeier. 1998. Nucleocytoplasmic transport: the soluble phase. *Annu. Rev. Biochem.* 67:265–306.

McBride, K.M., C. McDonald, and N.C. Reich. 2000. Nuclear export signal located within the DNA-binding domain of the Stat1 transcription factor. *EMBO J.* 19:6196–6206.

McBride, K.M., G. Banninger, C. McDonald, and N.C. Reich. 2002. Regulated nuclear import of the Stat1 transcription factor by direct binding of importin-alpha. *EMBO J.* 21:1754–1763.

Melén, K., L. Kinnunen, and I. Julkunen. 2001. Arginine/lysine-rich structural element is involved in interferon-induced nuclear import of STATs. *J. Biol. Chem.* 276:16447–16455.

Meyer, T., A. Begitt, I. Lödige, M. van Rossum, and U. Vinkemeier. 2002a. Constitutive and IFN-gamma-induced nuclear import of Stat1 proceed through independent pathways. *EMBO J.* 21:344–354.

Meyer, T., K. Gavenis, and U. Vinkemeier. 2002b. Cell type-specific and tyrosine phosphorylation-independent nuclear presence of Stat1 and Stat3. *Exp. Cell Res.* 272:45–55.

Meyer, T., A. Marg, P. Lemke, B. Wiesner, and U. Vinkemeier. 2003. DNA binding controls inactivation and nuclear accumulation of the transcription factor Stat1. *Genes Dev.* 17:1992–2005.

Meyer, T., L. Hendry, A. Begitt, S. John, and U. Vinkemeier. 2004. A single residue modulates tyrosine dephosphorylation, oligomerization, and nuclear accumulation of Stat transcription factors. *J. Biol. Chem.* 279:18998–19007.

Miller, M.W., M.R. Caracciolo, W.K. Berlin, and J.A. Hanover. 1999. Phosphorylation and glycosylation of nucleoporins. *Arch. Biochem. Biophys.* 367:51–60.

Miyamoto, Y., M. Hieda, M.T. Harreman, M. Fukumoto, T. Saiwaki, A.E. Hodel, A.H. Corbett, and Y. Yoneda. 2002. Importin alpha can migrate into the nucleus in an importin beta- and Ran-independent manner. *EMBO J.* 21: 5833–5842.

Nigg, E.A. 1997. Nucleocytoplasmic transport: signals, mechanisms and regulation. *Nature.* 386:779–787.

Paine, P.L., L.C. Moore, and S.B. Horowitz. 1975. Nuclear envelope permeability. *Nature.* 254:109–114.

Rodriguez, J.J., J.P. Parisien, and C.M. Horvath. 2002. Nipah virus V protein evades alpha and gamma interferons by preventing STAT1 and STAT2 activation and nuclear accumulation. *J. Virol.* 76:11476–11483.

Ryan, K.J., and S.R. Wente. 2000. The nuclear pore complex: a protein machine bridging the nucleus and cytoplasm. *Curr. Opin. Cell Biol.* 12:361–371.

Schwoebel, E.D., T.H. Ho, and M.S. Moore. 2002. The mechanism of inhibition of Ran-dependent nuclear transport by cellular ATP depletion. *J. Cell Biol.* 157:963–974.

Sekimoto, T., K. Nakajima, T. Tachibana, T. Hirano, and Y. Yoneda. 1996. Interferon-gamma-dependent nuclear import of Stat1 is mediated by the GTPase activity of Ran/TC4. *J. Biol. Chem.* 271:31017–31020.

Sekimoto, T., N. Imamoto, K. Nakajima, T. Hirano, and Y. Yoneda. 1997. Extracellular signal-dependent nuclear import of Stat1 is mediated by nuclear pore-targeting complex formation with NPI-1, but not Rch1. *EMBO J.* 16: 7067–7077.

Shuai, K., G.R. Stark, I.M. Kerr, and J.E. Darnell, Jr. 1993. A single phosphotyrosine residue of Stat91 required for gene activation by interferon-gamma. *Science.* 261:1744–1746.

Shuai, K., C.M. Horvath, L.H. Huang, S.A. Qureshi, D. Cowburn, and J.E. Darnell, Jr. 1994. Interferon activation of the transcription factor Stat91 involves dimerization through SH2-phosphotyrosyl peptide interactions. *Cell.* 76:821–828.

Vinkemeier, U., S.L. Cohen, I. Moarefi, B.T. Chait, J. Kuriyan, and J.E. Darnell, Jr. 1996. DNA binding of in vitro activated Stat1 alpha, Stat1 beta and truncated Stat1: interaction between NH2-terminal domains stabilizes binding of two dimers to tandem DNA sites. *EMBO J.* 15:5616–5626.

Zeng, R., Y. Aoki, M. Yoshida, K. Arai, and S. Watanabe. 2002. Stat5B shuttles between cytoplasm and nucleus in a cytokine-dependent and -independent manner. *J. Immunol.* 168:4567–4575.